Simultaneous Glint Spectral Signatures of Geosynchronous Satellites from Multiple Telescopes

Augustine J. DeMeulenaere, Eli Q. Harmon, and Francis K. Chun
Department of Physics, United States Air Force Academy

ABSTRACT

During glint season over the past three years, multiple teams of cadet space researchers have collected spectral measurements of geostationary satellites using the technique of slitless spectroscopy using a single telescope on the campus of the United States Air Force Academy. The spectral data collected over that time showed that the satellite solar panels are the source of the glints observed. When compared to a reflectance blackbody reference, the glint spectra exhibited strong absorption of photons on the red portion of the visible spectrum and shows a definite peak reflectance toward the blue end. This study continues on the previous work; however, this time we present measurements of glint spectra taken simultaneously from two separate telescopes, the Academy's on-campus 16-inch, f/8.2 telescope and the Academy's Falcon Telescope Network 20-inch, f/8.1 telescope located in Sterling, Colorado. The spectral data from the two different telescopes are compared to one another to determine similar features. Additionally, we analyze the measurements against reference blackbody to determine a relative percentage of solar energy absorbed by a satellite's solar panels.

1. BACKGROUND AND INTRODUCTION

An important mission for the United States Air Force that has become very apparent over the past 30 years is Space Situational Awareness (SSA). The Air Force has identified the space domain as a region becoming more congested, competitive, and contested. These characteristics of international competition for space superiority have driven the Air Force to be at the forefront of technology for purposes of national security. One mission crucial to this cause is space object characterization. Although the space-object catalogue maintains orbit data on approximately 22,000+ objects, there are many more unidentified objects that exist. More importantly there is concern of active satellites with unknown capabilities or supposedly inactive space objects suddenly coming back to life that threaten our national security. In order to combat this threat, the Air Force is developing various methods and strategies in order to increase SSA and have measurements to help characterize satellites. One particular area of research interest are geostationary satellites. Geostationary (GEO) satellites exist in an orbit containing the same angular velocity as the earth's rotation. Thus geostationary satellites remain at a fixed point on earth to more effectively conduct missions of communications, global positioning, weather forecasting, and remote sensing. Today there are around 400 geostationary satellites in use and this number is expected to only increase with time.

Over the past decade scientists have concerned themselves with identifying characteristics of a space object such as its attitude, material, surface composition, shape, and size. A high-resolution image of the space object aids in this characterization, however a dilemma we encounter is that most satellites, even the larger ones are either too far away or too small in size if close by. Fig. 1 below depicts this predicament which is termed non-resolvable space object identification (NRSOI).

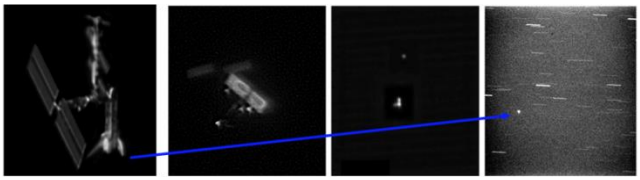

Fig. 1. Optical satellite image degrades with increasing distance and decreasing cross sectional size.

Standard astronomical measurements such as broadband photometry and spectroscopy have been used for NRSOI research. During the early years of the space age, researchers studied the properties associated with satellite optical detection, such as visibility, photometric orbit determination, and the temperature that a satellite reaches as a

result of radiation exchange with the environment [1-2]. Additionally, researchers also characterized satellites through the phenomenon of polarization [3] and studying the visible reflectance spectra [4]. Considerable progress has been made in satellite characterization using real and simulated photometry such as classification of GEO satellites and their glint signature [5-7], space debris optical characteristics [8-9], new techniques to separate attitude and shape information or determine basic satellite shape based on a satellite's light curve [10-11], and surface material characterization using multi-band optical signatures [12].

Spectral measurements have also been used to characterize satellites. Satellites exhibit a distinct reddening effect from space aging when compared to laboratory samples [13] or to measurements taken of the pre-flight satellite itself prior to launch [14]. Reflectance spectra of GEO debris also showed profile variations from night to night, but the overall shape of the spectrum seem to be conserved and could thus be used to derive surface materials [15]. However, caution must be taken when using reflectance spectra to inform operational conditions because the solar phase angle greatly impacts the observed spectrum and thus can limit analysis when combining measurements taken over different nights [16]. Obtaining spectra is easier now that the feasibility of slitless spectroscopy have been demonstrated [17] and refined [18]. Spectral measurements of GEO satellite glints have been observed and analyzed confirming that the source of the glint are the satellite solar panels [19].

Solar glints consist of the alignment of three components in order to be viewed: the sun, the satellite, and the observer on earth. These glints are a period of increased reflected sunlight where the observer is able to detect. Solar glints can occur at any time, but ground-based observers will only them during equinox periods [7]. Typically, a glint is a specular reflection off a surface, and thus usually resembles the source of the incident light [20]. For satellite glints, the source of incident light is the sun, which to first order is a blackbody emitter. Fig. 2 shows an example of a solar glint occurring on the Hubble Space Telescope's solar panels. This paper presents data and results taken of a particular GEO satellite during glint season simultaneously from two geographically separated telescopes, comparing those spectra to a blackbody spectra in an effort to determine relative power capacity. In this study, simultaneously simply means that the two telescopes observed the same object roughly during the same time period. No effort was made to synchronize the opening of the camera shutters by a hard trigger (e.g. GPS pulse) as that capability currently does not exist for either telescope.

Fig. 2. Solar glint on Hubble's solar panels. Image from *hubble.gsfc.nasa.gov*

2. INSTRUMENTATION

For this research we collected data from two telescopes located in Colorado (Fig. 3 and Table 1). The first telescope is a DFM Engineering f/8.2, 16-inch Ritchey-Chrétien system located at the USAFA Observatory. This telescope has an Apogee Alta U47 CCD camera with a 1024×1024 size focal plane and 13μm pixels, which provides a 0.23 degree (13 arc minutes on a side) field of view. This one has been used for the past four years of satellite

spectral research at USAFA, but now we are incorporating a second telescope in order to compare and contrast data taken simultaneously. The second telescope is located at Northeastern Junior College (NJC) in Sterling, Colorado and is part of the U.S. Air Force Academy's global Falcon Telescope Network (FTN) [21]. This telescope (NJC-Falcon) is a f/8.1, 20-inch Ritchey-Chrétien telescope, equipped with a similar, but newer model CCD camera, the Apogee Alta F47 also with a 1024×1024 size focal plane and 13μm pixels. The design of this telescope and camera provide slightly smaller field of view of 11 arc minutes. We use a nine-position filter wheel mounted in front of the cameras for both telescopes. This filter wheel houses a diffraction grating of 100 lines per millimeter in one of its slots (Fig. 4). The diffraction grating theoretical resolution is $103 < R < 147$ for a wavelength range of $350\ nm < \lambda$ $700\ nm$. The telescopes are separated by a distance of 232 kilometers or approximately 182 kilometers in latitude and 143 kilometers in longitude.

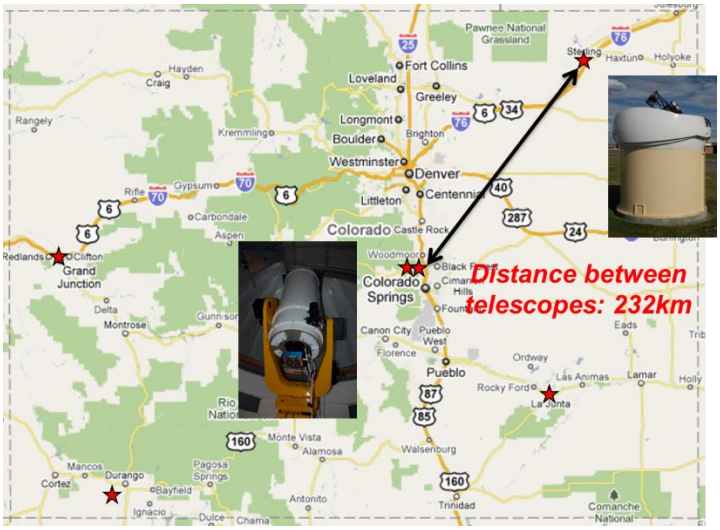

Fig. 3. Map showing the location of the two telescopes used in this study.

Table 1. Location of the two telescopes.

Education or Research Institute	City, State	Country	Longitude (east)	Latitude	Elevation (meters)	Avg Clear Nights per Year	Avg Sky Brightness at Zenith (mag/asec^2)
USAF Academy	Colorado Springs, CO	USA	255.12	39.01	2204	168	19
Northeastern Junior College	Sterling, CO	USA	256.80	40.65	1177	164	20

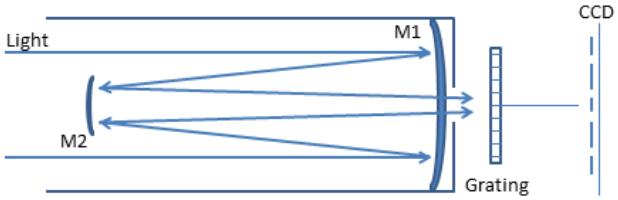

Fig. 4. Schematic of the slitless spectrograph used in this study.

We follow the processing procedures previously developed by USAFA cadets and faculty [18]. Data reduction involves rotating the images to align the spectra along the camera's focal plane, since the diffraction grating is

slightly misaligned with the focal plane. Next, the image is clipped to center it on the zeroth order location, and both bias and thermal noise corrections are made. All images that exhibit satellite spectra contaminated by star streaks or spectra are removed. Finally, a conversion is made from pixel-space to wavelength-space, with the two conversions for the respective telescopes listed here:

$$\lambda_{USAFA} = 1.646P + 5.752 \quad (1)$$

$$\lambda_{NJC} = 1.63P + 12.999 \quad (2)$$

where λ is the wavelength and *P* is the distance from the zeroth order spectra in pixels. The pixel-to-wavelength conversion is determined either by using Wolf-Rayet star emission lines and/or the absorption lines of standard stars (e.g. Alhena). The USAFA-16 conversion was already determined by a previous study [18], however the NJC-Falcon conversion was determined using absorption lines present in the spectra of the star Alhena (stellar classification A0 IV). The data used for the NJC-Falcon conversion is shown in Table 2 while Fig. 5 shows the spectra of Alhena in pixel space obtained by NJC-Falcon (left panel) and the calibrated spectra used to help us determine the pixel-to-wavelength conversion. It should be noted that although spectra were taken of solar analog stars each night of our observations, for the purpose of this initial study, no calibration of the satellite spectra with the solar analogs was applied.

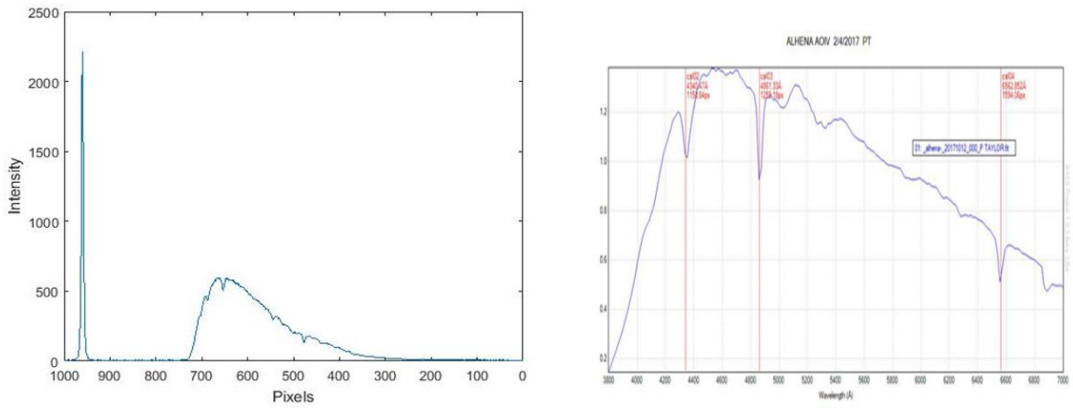

Fig. 5. Spectra of Alhena in pixel space taken by NJC-Falcon (left panel). Calibrated Alhena spectra used to determine the NJC-Falcon pixel-to-wavelength conversion (right panel).

Table 2: Pixel to Wavelength Conversion Data for NJC-Falcon

Alhena	
Pixel Delta	Wavelength (nm)
0	0
272	434
306	486
482	656

3. RESULTS AND ANALYSIS

In the weeks leading up to the Spring equinox, we observed the GEO satellite Wildblue-1 (satellite number 29643) twice on 6 and 15 March 2018 (Fig. 6). An example of simultaneous observations of Wildblue-1 (WB-1) taken by both telescopes on 6 March 2018 (UT: 0649-0709, 2018-03-07) is seen in Fig. 7. The left-hand spectral image was taken by the USAFA-16 telescope and the right-hand spectral image is from the remotely operated NJC-Falcon telescope. WB-1 is the brighter object in both images whereas the dimmer object is the satellite Anik-F2. The data is processed as discussed in the previous section and the resulting spectra are plotted as a function of time and wavelength where the x-axis is wavelengths in nanometers, the y-axis is time in seconds from the start of the

collection, and the z axis is the intensity of the spectra in counts per second. (Fig. 8). The left plots are the uncalibrated spectra measured by the USAFA-16 telescope (designated WB1-3) while the right plots are the uncalibrated spectra from the NJC-Falcon telescope (designated WB1-4). The bottom plots are the same as their respective top plots, but with a top-down perspective. The black trace is each plot indicates the wavelength corresponding to the peak intensity of each individual spectrum. It should be noted that Fig. 8 shows only a subset of data obtained that night from 0702-0709 UT, 2018-03-07, or approximately 7 minutes of data.

Fig. 6: Artist rendition of WildBlue-1 (image taken from Gunter's Space Page: http://space.skyrocket.de/doc_sdat/wildblue-1.htm)

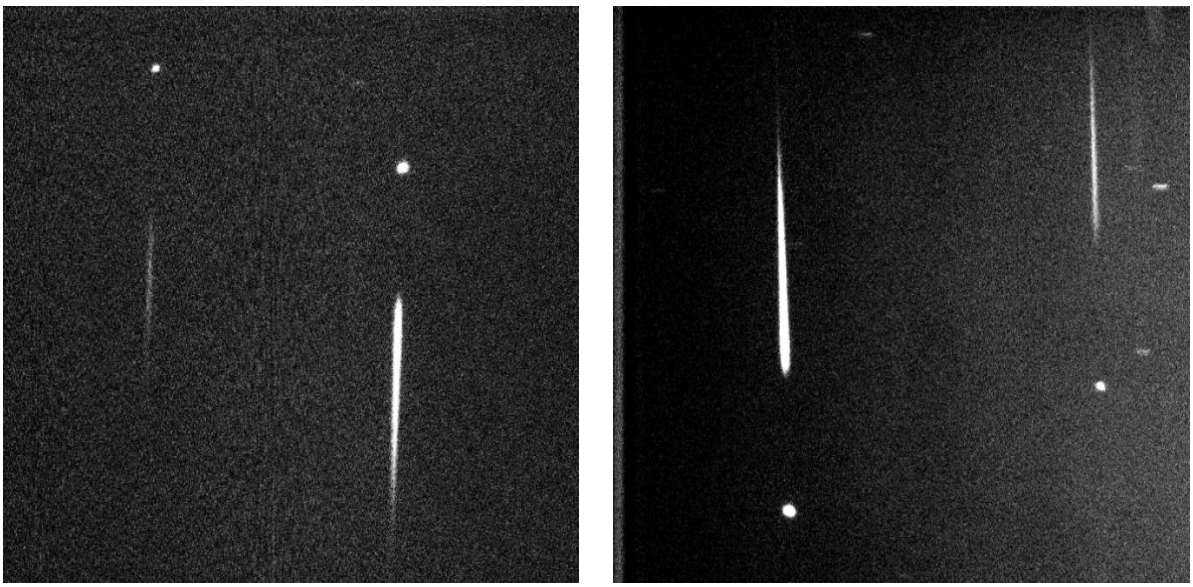

Fig. 7: Spectral image of WB-1 from USAFA-16 (left) and NJC-Falcon (right) telescopes. WB-1 is the brighter object in both images: right-side object in the left image and left-side object in the right image.

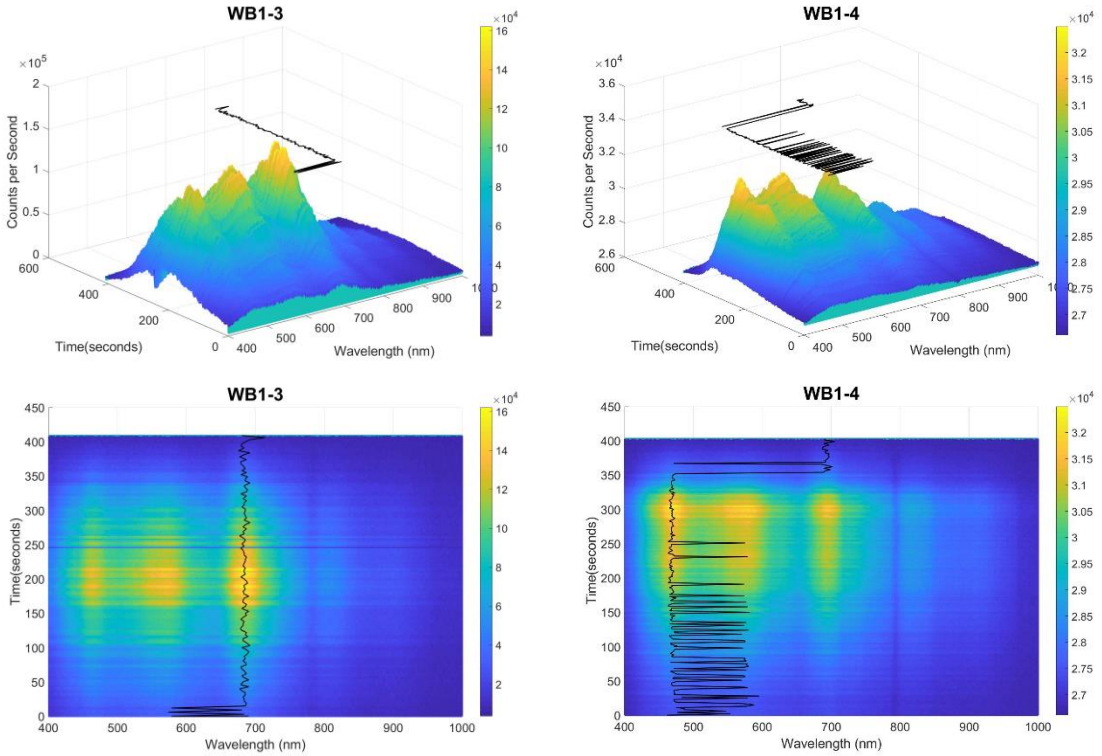

Fig. 8. Simultaneous spectra of WB-1 collected from 0702-0709 UT, 2018-03-07. Data on left is from USAFA-16 and on right is from NJC-Falcon.

The spectra collected on 6 March show WB-1 glinting between 150-250 seconds or approximately 0704-0706 UT (WB1-3) as observed by the USAFA-16 telescope and between 200-325 seconds or approximately 0705-0707 UT (WB1-4) as observed by the NJC-Falcon telescope. The glint is relatively intense on the order of 10^4-10^5 counts per second with USAFA-16 measuring a brighter relative glint. There are also three distinct peaks in the glint spectra centered on approximately 460 nanometers, 560 nanometers, and 690 nanometers. Interestingly, the longer wavelength peak is strongest in the WB1-3 data (USAFA-16) whereas the shorter wavelength peak is usually the strongest in the WB1-4 data (NJC-Falcon). The reason for this difference is currently unknown, however it could be simply due to a slight difference in solar illumination angles between the two telescope sites [16].

WB-1 was again observed spectrally simultaneously by USAFA-16 and NJC-Falcon 8 nights later early morning on 15 March 2018 (UT: 0643-0700, 2018-03-15), and the resulting spectra were definitely different than before (Fig. 9). The intensity of the glint observed on 14 March was much weaker than before by two orders of magnitude as USAFA-16 measured a 3,000 counts per second glint (WB1-5) while NJC-Falcon measured a 7,900 counts per second glint (WB1-6). And instead of a three-peak glint, both measured a single peak glint around 500 nanometers. The 15 March spectral observations appear similar to previous data collected on WB-1 by the USAFA-16 telescope on 23 February 2015 and 9 March 2016 which showed only a single peak between 480-620 nm [22]. A search of open source literature shows no major changes to WB-1's configuration or operations that can explain the different glint spectra. We could be observing reflections off different or multiple surfaces of the satellite; for instance, in addition to its large solar panel arrays, Wildblue-1 has a number of Ka-band dish antennae and other reflective surfaces that can glint (Fig. 6). This appears to support the premise that a thorough spectral characterization of a GEO object ideally requires measurements collected over the complete range of solar illumination geometries [16].

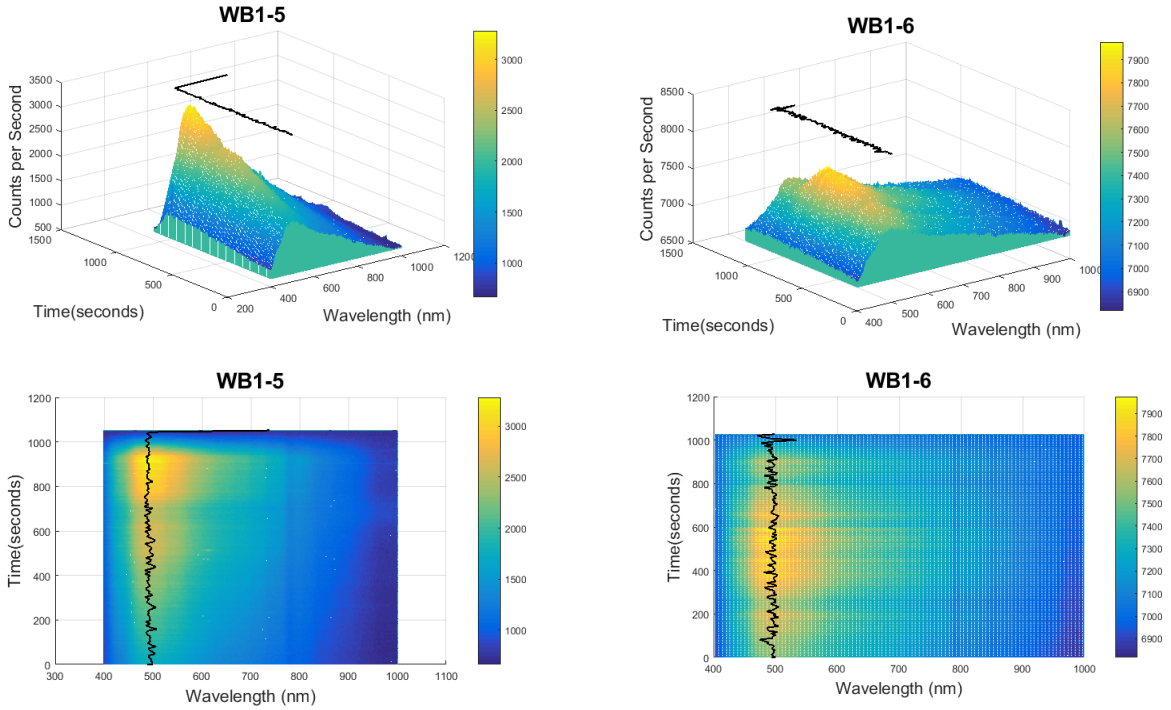

Fig. 9. Simultaneous spectra of WB-1 on 14 March 2018 (same format as Fig. 7).

We conducted a preliminary blackbody comparison of each respective observation split it into three phases: pre-glint, during glint, and post-glint when data were available. This was done in order to quantify the difference between the satellite spectra and a representative solar blackbody spectrum. The temperature of the blackbody was determined by applying Wien's Displacement Law corresponding to the wavelength associated with the average peak intensity before and after the glint period [19]. Fig. 10 shows analysis results for two different data collection periods, an earlier collection from a previous study and the 6 March 2018 collection (NOTE: analysis of the 15 March 2018 data was not attempted). The top panel of Fig. 10 is from 23 February 2015 previously analyzed by *Dunsmore et al*. [19]. The middle panel is the analysis for the spectra collected on 6 March by the USAFA-16 telescope, while the bottom panel is the analysis for the spectra collected by NJC-Falcon. There is no analysis conducted for the post-glint period of the 6 March 2018 collection due to the lack of measurements obtained.

The blue trace in each plot represents the average satellite spectra during the pre-, during, and post-glint periods, while the black trace depicts the blackbody reference. The blackbody reference curve is the same for all plots across a panel (pre-, during, and post-glint), but was scaled to match the peak of the appropriate satellite spectrum. This allowed us to determine a quantifiable difference between satellite and blackbody spectra using an absolute difference approach. Table 3 shows the quantitative absolute difference between the satellite spectra and the blackbody curve for all three events. The effective temperature calculated from the satellite spectra are also shown in the table (4727K, 5528K, and 5887K) which are reasonable when compared to the sun's effective blackbody temperature of 5800K. One can see that for the data collected by the USAFA-16 telescope, the during-glint spectrum is very different (~34-35%) than the other periods, especially the pre-glint period. This however is not the case for the spectral data collected by the NJC-Falcon telescope as the satellite spectrum pre- and during glint does not appear to resemble a blackbody. Further analysis of why this is the case is clearly warranted.

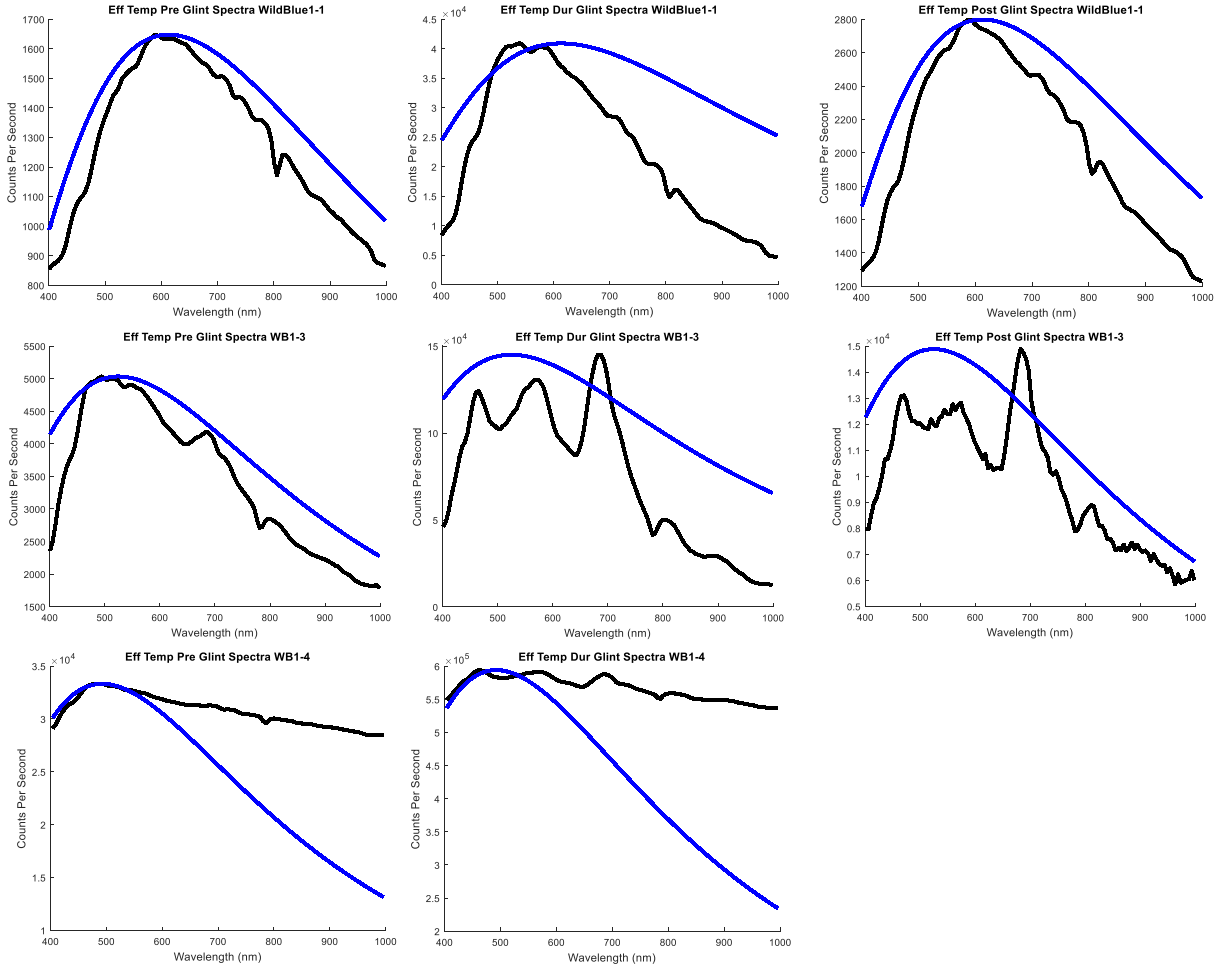

Fig. 10. Blackbody Analysis of WB-1 from USAFA-16 and NJC-Falcon. (Top data is from USAFA-16 taken 23 February 2015, Middle and bottom plots were taken 6 March 2018 from USAFA-16 and NJC-Falcon respectively.

Table 3. Blackbody Analysis Data of WB1-1, WB1-3, and WB1-4.

Data Set	**% Difference**
WB1-1 (23 February 2015), USAFA-16	T = 4727K
% of Blackbody (Pre-Glint)	8.1%
% of Blackbody (During Glint)	34.1
% of Blackbody (Post-Glint)	12.8
WB1-3 (6 March 2018), USAFA-16	T = 5528K
% of Blackbody (Pre-Glint)	12.3%
% of Blackbody (During Glint)	35.2%
% of Blackbody (Post-Glint)	16.8%
WB1-4 (6 March 2018), NJC-Falcon	T = 5887K
% of Blackbody (Pre-Glint)	24.5%
% of Blackbody (During Glint)	28.3%
% of Blackbody (Post-Glint)	N/A

4. CONCLUSIONS

We present what we believe for the first time are simultaneous spectral data of satellite glints from two different telescopes, one located on campus at the United States Air Force Academy and one located 232 kilometers away in Sterling, Colorado. The spectral measurements show relative consistency between telescopes as they observed the GEO satellite Wildblue-1. However, there were differences in the glint spectra between the two nights of collection, both in relative intensity and profile. This supports the premise that solar illumination angles play a major role in observed spectral signatures [16]. Although it appears that the glint is solar panel related, other spacecraft surfaces could be specularly reflecting as well. Clearly more data is required, especially simultaneous observations. Finally, as this study reports the first spectral measurements from one of the Falcon telescopes, data reduction and processing of that system's data needs refinement. However, simultaneous satellite observations offer the promise of advancing out capabilities in space object characterization in support of the space situational awareness mission area.

5. ACKNOWLEDGEMENTS

The authors would like to acknowledge support by the United States Air Force Academy and the Air Force Office of Scientific Research.

6. REFERENCES

[1] Tousey, R., "Optical Problems of the Satellite," *Journal of the Optical Society of America*, Vol. 47, No. 4, April 1957, pp. 261-267

[2] Kissell, K.E. and Tyson, E.T., "Rapid-Response Photometry of Satellites," *Astronomical Journal*, Vol. 69, p. 547 (1964).

[3] Stead, R.P., "An Investigation of Polarization Phenomena Produced by Space Objects," M.S. Thesis, GSP/PH/67-7, Air Force Institute of Technology, Wright-Patterson Air Force Base, Ohio, 1967.

[4] Lambert, J.V., "Measurement of the Visible Reflectance Spectra of Orbiting Satellites," *M.S. Thesis*, Air Force Institute of Technology, Dayton, OH, March 1971.

[5] Payne, T. E., Gregory, S. A., Houtkooper, N. M., and Burdullis, T. W., "Classification of Geosynchronous Satellites Using Photometric Techniques", Proceedings of the 2002 AMOS Technical Conference, The Maui Economic Development Board, Inc., Kihei, Maui, HI, 2002.

[6] Payne, T. E., Gregory, S. A., and Luu, K., "SSA Analysis of GEOS Photometric Signature Classifications and Solar Panel Offsets," *Proceedings of the 2006 AMOS Technical Conference*, The Maui Economic Development Board, Inc., Kihei, Maui, HI, 2006, pp. 667-673.

[7] Vrba, F.J., DiVittorio, M.E., Hindsley, R.B., Schmitt, H.R., Armstrong, J.T., Shankland, P.D., Hutter, D.J., and Benson, J.A., "A survey of geosynchronous satellite glints." The 2009 AMOS Technical Conference Proceedings, The Maui Economic Development Board, Inc., Kihei, Maui, HI, 2009.

[8] Schildknecht, T., Musci, R., Flury, W., Kuusela J., de Leon, J., and de Fatima Dominguez Palmero, L., "Properties of High Area-to-Mass Ratio Space Debris Population in GEO," *The 2005 AMOS Technical Conference Proceedings*, The Maui Economic Development Board, Inc., Kihei, Maui, HI, 2005, pp. 216-223.

[9] Seitzer, P., Abercromby, K.J., Barker E.S., and Rodriguez H.M., "Optical Studies of Space Debris at GEO - Survey and Follow-up with Two Telescopes," *Proceedings of the 2007 AMOS Technical Conference*, The Maui Economic Development Board, Inc., Kihei, Maui, HI, 2007, pp. 338-343.

[10] Hall, D., Calef, B., Knox, K., Bolden, M., and Kervin, P., "Separating Attitude and Shape Effects for Non-resolved Objects," *The 2007 AMOS Technical Conference Proceedings*, The Maui Economic Development Board, Inc., Kihei, Maui, HI, 2007, pp. 464-475.

[11] Daniel O. Fulcoly, Katharine I. Kalamaroff, and Francis K. Chun, "Determining Basic Satellite Shape from Photometric Light Curves," Journal of Spacecraft and Rockets, vol. 49, no. 1, Feb. 2012.

[12] Hall, D., Hamada, K., Kelecy, T., and Kervin, P., "Surface Material Characterization from Non-resolved Multi-band Optical Observations," *The 2012 AMOS Technical Conference Proceedings*, The Maui Economic Development Board, Inc., Kihei, Maui, HI, 2012, pp. 200-209.

[13] Jorgensen, K., Okada, J., Africano, J., Hall, D., Guyote, M., Hamada, K., Stansbery, G., Barker, E., and Kervin, P., "Reflectance Spectra of Human-Made Space Objects," *The 2004 AMOS Technical Conference Proceedings*, The Maui Economic Development Board, Inc., Kihei, Maui, HI, 2004, pp. 42-51.

[14] Abercromby, K.J., Hamada, K., Guyote, M., Okada, J., Barker, E., "Remote and Ground Truth Spectral Measurement Comparisons of FORMSAT III," *The 2007 AMOS Technical Conference Proceedings*, The Maui Economic Development Board, Inc., Kihei, Maui, HI, 2007, pp. 379-388.

[15] Schildknecht, T., Vananti, A., Krag, H., and Erd, C., "Reflectance spectra of space debris in GEO," *The 2009 AMOS Technical Conference Proceedings*, The Maui Economic Development Board, Inc., Kihei, Maui, HI, 2009, pp. 220-227.

[16] Bédard, D., Wade, G., Monin, D., and Scott, R., "Spectrometric characterization of geostationary satellites," Proceedings of the 2012 AMOS Technical Conference, The Maui Economic Development Board, Inc., Kihei, Maui, HI, 2012.

[17] Hoag, A. and Schroeder, D., "Nonobjective grating spectroscopy", Publications of the Astronomical Society of the Pacific, Vol. 82, No. 489 (October 1970), pp. 1141-1145.

[18] Tippets, R.D., Wakefield, S., Young, S., Ferguson, I., Earp-Pitkins, C., and Chun, F.K., "Slitless spectroscopy of geosynchronous satellites," *Opt. Eng*. 54(10), 104103 (2015). doi: 10.1117/1.OE.54.10.104103.

[19] Dunsmore, A.N., J.A. Key, R.M. Tucker, E.M. Weld, F.K. Chun, and R.D. Tippets, "Spectral Measurements of Geosynchronous Satellites During Glint Season," *J. Spacecraft and Rockets*, 7 October 2016. doi: http://arc.aiaa.org/doi/abs/10.2514/1.A33583.

[20] Cook, R.L and Torrance, K.E., "A Reflectance Model for Computer Graphics", *ACM Transactions on Graphics*, Vol.1, 7-24, 1982.

[21] Francis K. Chun *et al* 2018 *PASP* **130** 095003.

[22] Weisz, D.E. and F.K. Chun, "Comparison of Geosynchronous Satellites Spectral Signatures During Glint Season," *The 2017 AMOS Technical Conference Proceedings*, The Maui Economic Development Board, Inc., Kihei, Maui, HI, 2017, pp. 1332-1348.